Influence of the pentaerythritol phosphate melamine salt content on the combustion and thermal decomposition process of intumescent flame-retardant ethylene–vinyl acetate copolymer composites

Feng Zhang,[1] Wenying Sun,[1] Yong Wang,[1] Bensheng Liu[2]

[1]College of Environment and Safety Engineering, Qingdao University of Science and Technology, 53 Zhengzhou Road, Qingdao 266042, People's Republic of China
[2]Qingdao Fire Detachment, 16 Jinhu Road, Qingdao 266071, People's Republic of China
Correspondence to: F. Zhang (E-mail: zhangfengqd@163.com)

ABSTRACT: Pentaerythritol phosphate melamine salt (PPMS) as a single-molecule intumescent fire retardant was synthesized and characterized. The influence of the PPMS content on the combustion and thermal decomposition processes of intumescent-flame-retardant (IFR) ethylene–vinyl acetate copolymer (EVA) composites was studied by limiting oxygen index (LOI) measurement, UL 94 rating testing, cone calorimetry, thermogravimetric analysis, and scanning electron microscopy. The LOI and UL 94 rating results illustrate that PPMS used in EVA improved the flame retardancy of the EVA composites. The cone calorimetry test results show that the addition of PPMS significantly decreased the heat-release rate, total heat release, and smoke-production rate and enhanced the residual char fire performance of the EVA composites. The IFR–EVA3 composite showed the lowest heat-release and smoke-production rates and the highest char residue; this means that the IFR–EVA3 composite had the best flame retardancy. The thermogravimetry results show that the IFR–EVA composites had more residual char than pure EVA; the char residue yield increased with increasing PPMS content. The analysis results for the char residue structures also illustrated that the addition of PPMS into the EVA resin helped to enhance the fire properties of the char layer and improve the flame retardancy of the EVA composites. © 2015 Wiley Periodicals, Inc. J. Appl. Polym. Sci. 2015, 132, 42148.

INTRODUCTION

Polyethylenic polymers have been widely used in many fields, including infrastructure applications, such as in chemical plants, civil buildings, and other facilities. However, most polymers are flammable because of their chemical constitution, and flame retardancy is usually required in these applications.[1–6] Morgan and Gilman[7] reviewed the progress of commercial flame-retardant technology. They explained the reason why flame retardants are widely used nowadays and how they are applied.

Ethylene–vinyl acetate copolymer (EVA) resin, as a kind of widely used polyethylenic polymer, is copolymerized by ethylene and vinyl acetate ions. At the same time, EVA is also flammable [its limiting oxygen index (LOI) is only about 18], and this limits its further application. It is well known that halogen-containing fire retardants are effective for EVA polymer materials; the environmental damage problems accompanied by these flame retardants are unacceptable nowadays, and this has limited their further use on many occasions. As an alternative method for improving the polymer's fire resistance, the use of intumescent fire-retardant systems is growing rapidly.[8–11]

Intumescent flame retardants (IFRs) are halogen free; they provide flame-retardancy properties by forming a char layer on the surface and protecting the substrate from outer heat flux. The resulting char can reduce heat transfer to the underlying material. The intumescence concept allows a balance between the fire properties and the level of additives in the material.[12–14]

Camino and Luda[15] also reviewed the progress of the intumescence mechanisms of intumescent fire-retardant systems. Bras and Bourbigot[16] did some research on an ammonium polyphosphate/pentaerythritol/melamine system and completed a review about intumescent fire-retardant thermoplastic formulations, their synergy, and their synergistic agents. However, there exist some problems in these polyol-type carbonization agents; these include exudation and water solubility. In addition, they are incompatible with the polymeric matrix, and this weakens the mechanical properties of the material. So, much attention has
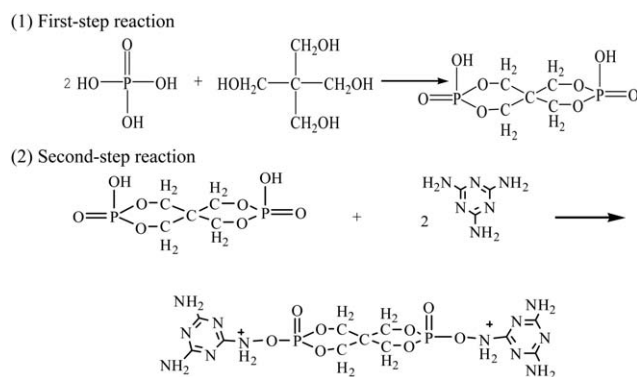
Scheme 1. The reaction synthesis route of PPMS.

been concentrated on investigating other carbonization agents.[17] Alongi et al.[18] used expandable graphite and poly(ethylene terephthalate) to develop a new nanocomposite IFR, which had good flame retardancy when applied to plastics and textiles. In particular, intumescent mixtures of the additives ammonium polyphosphate and polyamide 6 were developed for use in polypropylene (PP) and EVA copolymers.[19]

In recent years, many IFRs have been synthesized and used in polymers. Liu et al.[17] developed a novel IFR containing ammonium polyphosphate and poly(tetramethylene terephthalamide); it was prepared as a flame-retardant acrylonitrile–butadiene–styrene. Among these synthesized flame retardants, synthesized IFRs containing an acid source, carbon source, and gas source have attracted researchers' interest; they are halogen-free and have a high efficiency, environmentally protective qualities, and good compatibility. At the same time, they do little damage to the mechanical properties of the matrix material. However, IFR mechanisms are quite complicated,[20–22] and there may be different mechanisms with different matrix resins and different flame retardants; these still need to be studied further and understood.

In this study, a single-molecule intumescent fire retardant, PPMS, was synthesized with phosphorus acid, melamine, and pentaerythritol. The structure of PPMS is characterized by Fourier transform infrared (FTIR) spectroscopy, elemental analyses, ^{1}H-NMR spectra, and [13]P-NMR spectra. The influence of the PPMS content on the combustion and thermal decomposition processes of the IFR–EVA composites were studied by LOI measurement, UL 94 rating testing, cone calorimetry, and thermogravimetric analysis. The char residues after combustion were investigated with scanning electronic microscopy.

EXPERIMENTAL

Materials
Pentaerythritol was supplied by Tianjin Guangfu Co., Ltd. (China). Phosphoric acid was made by Laiyang Fine Chemical Factory (China). Anhydrous aluminum chloride was supplied by Tianjin Damao Chemical Reagent Factory (China). Methyl benzene was manufactured by Yantai Sanhe Chemical Reagent Co., Ltd. (China). Melamine was provided by Shanghai Aibi Chemistry Preparation Co., Ltd. (China). Finally, EVA (EVA-83) was prepared by Beijing Eastern Petrochemical Co., Ltd. (China).

Synthesis of the Single-Molecule Intumescent Fire Retardant
PPMS, which is a single-molecule intumescent fire retardant, was synthesized in our laboratory on the basis of phosphorus acid, melamine, and pentaerythritol.

Amounts of 68 g of pentaerythritol, 96 mL of phosphoric acid, 3 g of anhydrous aluminum chloride, and 150 mL of methylbenzene were added to a three-necked, round-bottomed flask equipped with a mechanical stirrer, condenser, and thermometer. The mixture was heated at 85°C in an oil bath at a stirring rate of 320 rpm for 7.5 h; then, 50 mL of methylbenzene was added to a three-necked, round-bottomed flask to react for 0.5 h under the same conditions. Heating was stopped with a stirring rate of 200 rpm. Then, excess methyl benzene was distilled from the three-necked, round-bottomed flask, and a yellow glue chemical appeared. Then, 59.6 g of melamine and 300 mL of distilled water were added to the previous three-necked, round-bottomed flask. After completion of the melamine and water addition, the reaction mixture was maintained at a temperature of 120°C in an oil bath with a stirring rate of 320 rpm for 1 h. At last, the IFR was obtained after the suspension was filtered and dried.

The reaction synthesis route of PPMS is shown in Scheme 1.

Sample Preparation
The materials used to prepare the IFR–EVA composites included EVA and PPMS, which were dried at 60°C for 3 h. Certain amounts of EVA and PPMS were weighed separately with an electronic balance. After EVA was heated to the melting state in an internal mixer (SU-70B, Changzhou Suyan Science and Technology Co., Ltd., China), PPMS was mixed with the EVA polymer in mixer at a temperature of 130°C for 15 min to obtain the IFR–EVA compounds based on the different formulations. At last, each of the compounds was compressed at 145°C under 20 MPa for 30 min to obtain a specimen sheet with dimensions of $100 \times 100 \times 3$ mm^3 with a hot press machine (ZG-10T, Dongguan Zhenggong Electromechanical Equipment Technology Co., Ltd., China). The formulations of the IFR–EVA composites are listed in Table I.

Measurements
Elemental analyses (C, H, N, S, and O) of PPMS were obtained with a Vario EL analyzer (Hanau, Germany). A combustion method was used to determine the C, H, and N contents while the sample was pyrolyzed in an oxygen flow.

IR spectra were obtained from KBr pellets on a Bruker Tensor 27 Fourier transform infrared spectrometer in the $400–4000\text{-}cm^{-1}$ region.

^{1}H-NMR spectra and [13]P-NMR spectra were recorded on a Bruker AV400 (400-MHz) spectrometer.

An HC-2 oxygen index meter (Jiangning Analysis Instrument Co., China) was used to measure the LOI value of the IFR–EVA

Table I. Formulations of the IFR–EVA Composites

Sample code	EVA (mass %)	PPMS (mass %)
EVA	100	0
IFR–EVA-1	80	20
IFR–EVA-2	70	30
IFR–EVA-3	60	40

Table II. LOI Values and UL 94 Testing Results for IFR–EVA Composites

Sample code	PPMS (mass %)	LOI	UL-94 rating
EVA	0	17.1	No rating
IFR-EVA-1	20	22.5	V-2
IFR-EVA-2	30	27.7	V-0
IFR-EVA-3	40	29.3	V-0

composites according to ASTM D 2863. The specimens used for the tests had dimensions of $100 \times 6.5 \times 3$ mm^3.

A CFZ-2-type instrument (Jiangning Analysis Instrument Co., China) was used to conduct the vertical test according to the American National Standard UL-94 standard. The specimens used had dimensions of $130 \times 13 \times 3$ mm^3.

An FTT cone calorimeter (Fire Testing Technology, Ltd., United Kingdom) was used to evaluate the combustion behavior of the IFR–EVA coatings according to the procedure defined in ISO-5660-1.The standard procedure used involved the exposure of the specimens at heating flux levels of 50 kW/m^2, and the specimen sizes were $100 \times 100 \times 3$ mm^3.

Thermogravimetric analysis was examined on a DT-50 (Setaram, France) instrument under nitrogen flow at 5 mL/min. About 10.0 mg of sample was put in an alumina crucible and heated from 25 to 800°C. The heating rate was set as 10 K/min.

Melting points were determined on an X-4 micromelting point apparatus (Shanghai PSE Co., Ltd., China).

RESULTS AND DISCUSSION

Characterization of PPMS

The measurement of the melting points for the PPMS sample showed that the melting point was in the range 327–335°C. Elemental analyses indicated that the C, N, and H contents of the PPMS sample were 30.57, 31.18, and 3.34%, respectively; these values were basically consistent with the theoretical values (29.32, 31.57, and 3.38%, respectively). Figure 1 shows the FTIR spectra obtained from the PPMS sample. As shown in the figure, the relative absorption peaks appeared at 1240–1370 cm^{-1} and were mainly due to P=O group vibration. The absorption peaks appeared at 2850–3200 cm^{-1} and could be attributed to CH$_3$ or CH$_2$ group vibration. There were also some absorption peaks occurring at 600–1100 cm^{-1}; these were due to the vibration of the spirane structure. The absorption peak at 3470 cm^{-1} was mainly due to NH$_2$ group vibration. The absorption peak at 1520–1670 cm^{-1} was mainly due to C=N group vibration.

The ^{1}H-NMR and ^{13}P-NMR spectra of PPMS prepared in our laboratory are displayed in Figure 2. As shown in the ^{1}H-NMR spectra [Figure 2(a)], there were three strong signals that represented the three types of H atom ($\delta = 2.3$, 3.2, and 6.7). The signals were consistent with the structural formula of PPMS, which were H atoms from —NH$_3$ in the melamine ring, H connected to phosphate ester groups, and H from —CH$_2$ in spirocyclic pentaerythritol, respectively. There was only one strong signal ($\delta = 0.532$) in the ^{13}P-NMR spectra [Figure 2(b)], which indicated the same chemical structure for these P atoms in PPMS.

All of these characterization results of PPMS prepared in our laboratory indicated that the synthesized single-molecule intumescent fire retardant was consistent with the chemical's structural formula.

LOI and UL 94 Rating

Table II presents the LOI values and UL94 testing results of the EVA and IFR–EVA composites. The LOI values of the IFR–EVA composites increased with increasing PPMS content. The LOI value of the composite containing 40% PPMS reached 29.3. The UL 94 ratings of the IFR–EVA composites also increased with increasing PPMS content. A V-0 rating was achieved when the PPMS content was 30 or 40%; this indicated reduced flame spread during burning. The previous results illustrate that the PPMS used in EVA could improve the flame retardancy of the composites (both in the LOI value and UL-94 rating).

Cone Calorimetry Study

LOI and UL-94 tests are widely used to evaluate the flame retardancy of materials; this also helps to select the best appropriate flame-retardant formulation for polymers. However, cone calorimetry provides a more real fire experiment scenario for analyzing the burning behavior of materials. Some cone calorimeter results have been found to correlate well with those obtained from large-scale fire tests, and these can be used to predict the behavior of materials in real fires. Heat-release rate (HRR) measurement is based on the oxygen consumption principle.[23]

Figure 3 shows the HRR curves of the pure EVA and IFR–EVA composites with different PPMS contents obtained from the cone calorimetry test. As shown in Figure 1, the pure EVA material burned very fast after ignition, and a sharp HRR peak appeared. In the case of the IFR–EVA composites, their peak heat release rate (PHRR) values were greatly reduced and decreased with increasing PPMS content, as shown in Table III. The PHRR values of the pure EVA, IFR–EVA1, IFR–EVA2, and IFR–EVA3 composites were 1688, 337, 291, and 235 kW/m^2, respectively. Accordingly, PHRR was reduced by about 80, 83, and 86% in the IFR–EVA1, IFR–EVA2, and IFR–EVA3 samples, respectively. Moreover, the combustion process of the IFR–EVA composites was prolonged in comparison with that of the pure
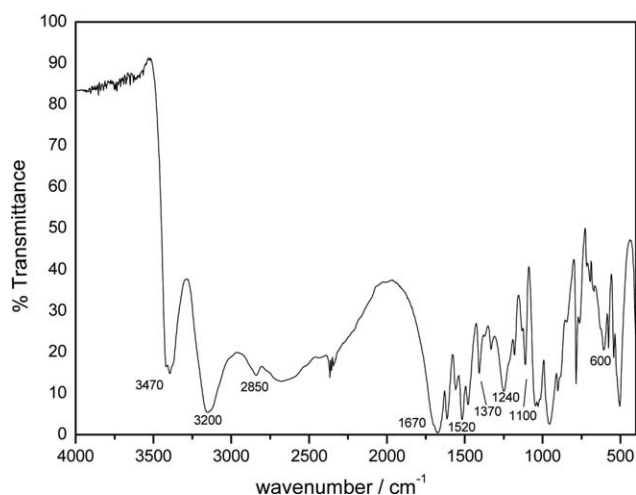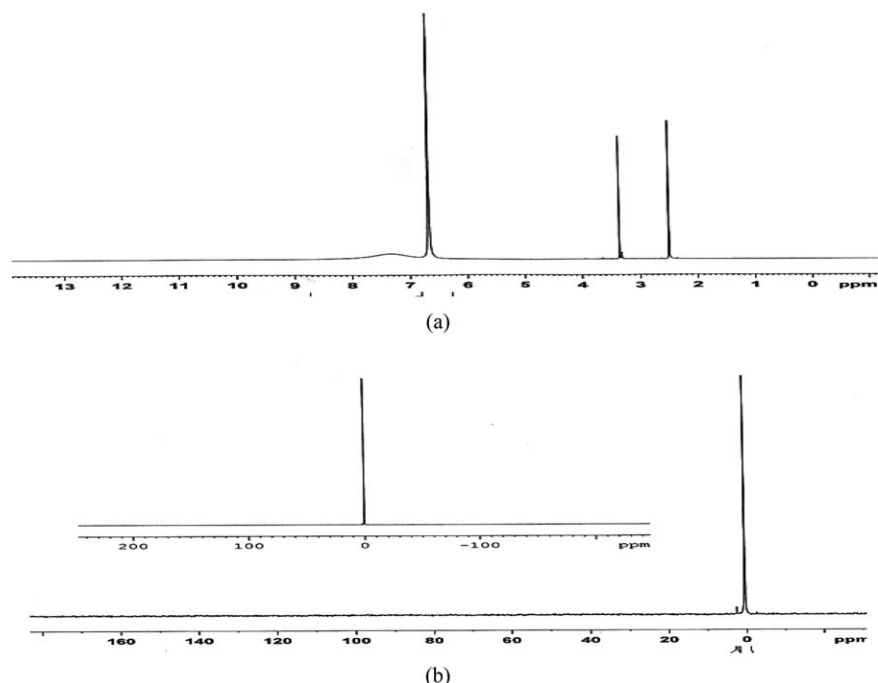

Figure 1. FTIR spectra of PPMS.

Figure 2. NMR spectra for PPMS: (a) ^{1}H-NMR for PPMS and (b) ^{31}P-NMR for PPMS.

EVA material. The combustion behaviors of the EVA and IFR–EVA materials were also investigated in previously reported studies.[19,20] The PHRR values of EVA and IFR–EVA made by Bras and Bourbigot[19] were about 1800 and 400 kW/m^2, respectively. Thus, PHRR was reduced by about 78% from EVA to the IFR–EVA materials; this was lower than that of our IFR–EVA materials. At the same time, the IFRs used by Bras and Bourbigot were ammonium polyphosphate and polyamide 6, which could not overcome the bad compatibility of ammonium polyphosphate and EVA. The IFR used here was a single molecule, which was synthesized on the basis of phosphorus acid, melamine, and pentaerythritol and had good compatibility with EVA. Thus, the IFR–EVA composites made by our laboratory showed a better performance, such as with the flame retardancy, than the IFR–EVA composites made by Bras and Bourbigot.

The total heat release (THR) is a parameter that determines how large a fire is. Once the ignition happens, THR steadily increases with burning time and reaches a steady state before flameout occurs. THR is often used as a measurement of the propensity to sustain a fire for a long duration.[24] An efficient flame-

Table III. PHRR of the Pure EVA and IFR–EVA Composites

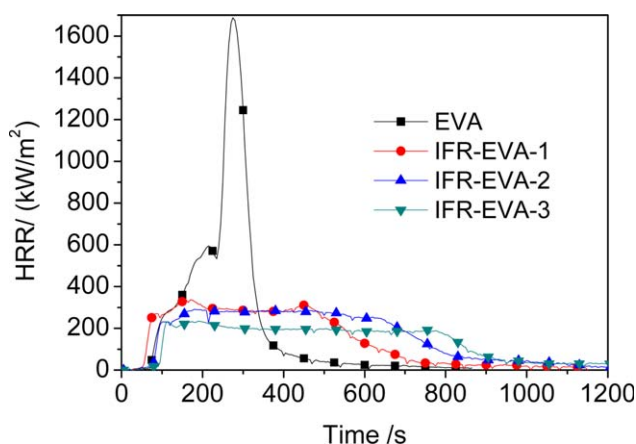| Sample code	PPMS (mass %)	PHRR (kW/m^2)
EVA	0	1688
IFR–EVA-1	20	337
IFR–EVA-2	30	291
IFR–EVA-3	40	235

Figure 3. HRRs of the EVA and IFR–EVA composites at an incident heat flux of 50 kW/m^2. [Color figure can be viewed in the online issue, which is available at wileyonlinelibrary.com.]
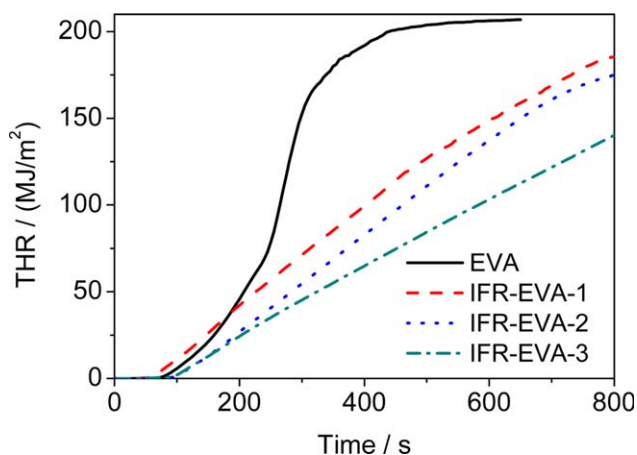

Figure 4. THR rates of the EVA and IFR–EVA composites at an incident heat flux of 50 kW/m^2. [Color figure can be viewed in the online issue, which is available at wileyonlinelibrary.com.]

Table IV. TG and DTG Data for the Pure EVA and IFR–EVA Composites

Sample code	$T_{0.1}$ (°C)	$T_{0.5}$ (°C)	$\Delta T_{0.1–0.5}$ (°C)	R_{max1} (%/min)	R_{max2} (%/min)	T_{max1} (°C)	T_{max2} (°C)	ε (%)
EVA	362.0	464.9	102.9	0.00278	0.0227	351.8	473.3	1.44
IFR-EVA-1	348.9	460.9	112.0	0.00252	0.0165	348.3	472.5	6.38
IFR-EVA-2	341.6	461.2	119.6	0.00298	0.0157	359.1	473.2	11.69
IFR-EVA-3	337.8	461.3	123.5	0.00350	0.0138	384.7	472.9	12.13

retardant should have the ability to reduce THR effectively when it is incorporated into a polymer. As shown in Figure 4, THR WAS progressively reduced with increasing PPMS content. At 400 s after the application of the external heat flux during the cone calorimeter test, the THR values of the pure EVA, IFR–EVA1, IFR–EVA2, and IFR–EVA3 composites were 192, 99, 83, and 65 MJ/m^2, respectively. Accordingly, THR was reduced by about 48, 57, and 66% in the IFR–EVA1, IFR–EVA2, and IFR–EVA3 samples, respectively. The THR of the IFR–EVA composites with PPMS flame retardant showed a different degree of reduction than the pure EVA without any flame additives under the same experimental conditions; this may have been due the fact that there was a lot of char residue formed in the case of the sample with PPMS.

The smoke-production rate (SPR) is an important smoke measurement parameter. SPR is the ratio of the specific extinction area to the mass loss rate. It is the area of obscuration produced per second (square meters per second). To some extent, SPR can also be used to evaluate the flame retardancy of materials.[25]

Figure 5 illustrates the effect of the PPMS content on the reduction of the SPR of IFR–EVA composites at an incident heat flux of 50 kW/m^2. As shown in Figure 5, the PPMS flame retardant significantly suppressed the SPR of the EVA composites. The SPR peak of EVA (0.062 m^2/s) was the highest among all of the samples. At the same time, SPR decreased with increasing PPMS content. The SPR curves of IFR–EVA1, IFR–EVA2, and IFR–EVA3 proceeded similarly, reached a peak rapidly first, and then tended to be flat. The reason was the formation of a char layer on the surface of the samples, which suppressed the fire spread and limited the production of smoke.
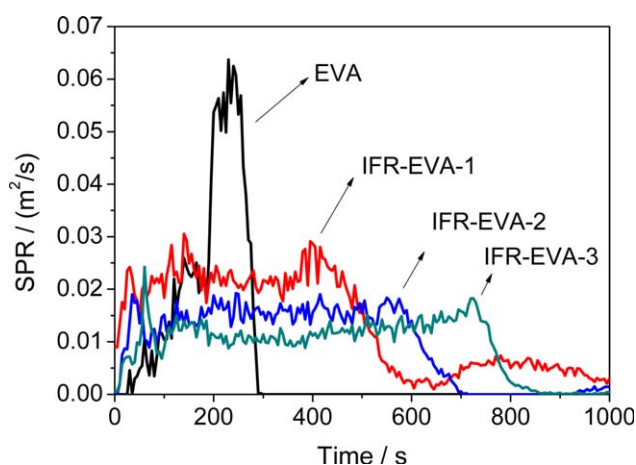
Thermal Stability Analysis

To examine the effect of the PPMS content on the thermal stability and decomposition behavior, thermogravimetric analysis data under nitrogen atmospheres were determined and analyzed. Some data of key parameters, such as the degradation temperature, the temperature at which 10.0% mass loss occurs ($T_{0.1}$), the temperature at which 50.0% mass loss occurs ($T_{0.5}$), the temperature difference ($\Delta T_{0.1–0.5}$; i.e., $\Delta T_{0.1–0.5} = T_{0.5} - T_{0.1}$), the maximum mass loss rate in the first degradation stage (R_{max1}), the maximum mass loss rate in the second degradation stage (R_{max2}), the temperature at which R_{max1} occurs (T_{max1}), the temperature at which R_{max2} occurs (T_{max2}), and the residual char yield at 800°C, are listed in Table IV.

Figure 5. SPRs of the pure EVA and IFR–EVA composites at a flux of 50 kW/m^2. [Color figure can be viewed in the online issue, which is available at wileyonlinelibrary.com.]
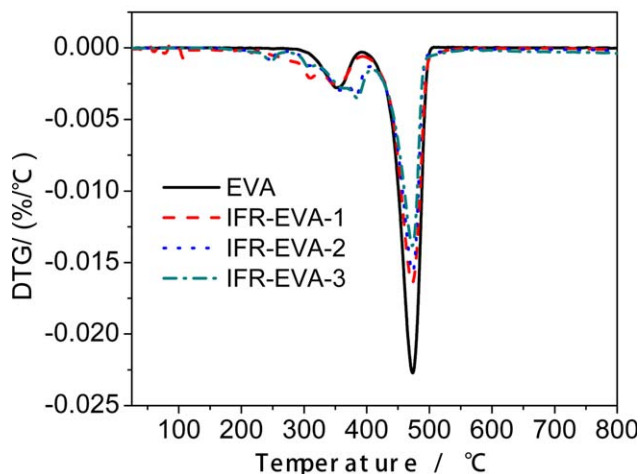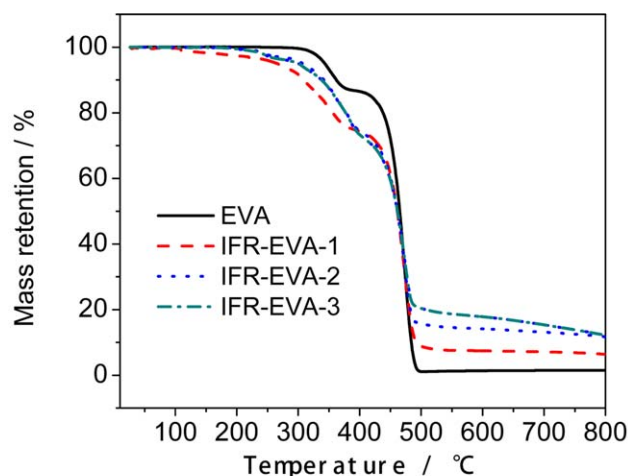
Figure 6. TG and DTG curves of the pure EVA and IFR–EVA composites. [Color figure can be viewed in the online issue, which is available at wileyonlinelibrary.com.]
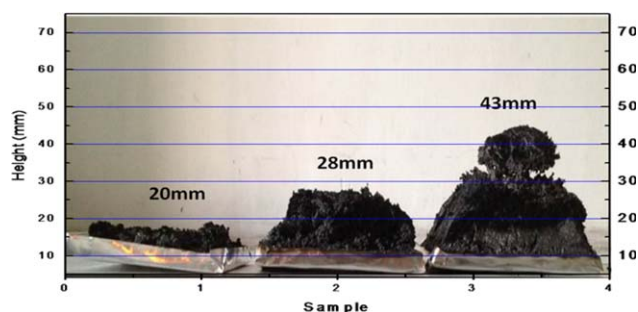
Figure 7. Residual char after the burning of IFR–EVA1 (sample 1), IFR–EVA2 (sample 2), and IFR–EVA3 (sample 3). [Color figure can be viewed in the online issue, which is available at wileyonlinelibrary.com.]

Figure 6 shows the thermogravimetry (TG) and differential thermogravimetry (DTG) curves of the pure EVA and IFR–EVA composites. As shown in Figure 6 and Table IV, the pure EVA and IFR–EVA composites all had two mass loss stages. For IFR–EVA1, the PPMS content was 20%, and the first degradation region mainly occurred between 109.5 and 382.7°C. $T_{0.1}$ of IFR–EVA1 was 348.9°C, which was lower than that of pure EVA. In the degradation process, the IFR–EVA1 composite decomposed faster than pure EVA because of the lower thermal stability of the P—O—C structure in IFR; this could degrade into poly(phosphoric acid) and catalyze EVA degradation. R_{max2} of IFR–EVA1 was also lower

than that of pure EVA. The char yield (ε) of IFR–EVA1 at 800°C was about 6%, which was higher than that of pure EVA (ca. 1%).

The TG and DTG curves of IFR–EVA2 and IFR–EVA3 proceeded similarly to that of IFR–EVA1. The $T_{0.1}$ values of the IFR–EVA2 and IFR–EVA3 were 341.6 and 337.8°C; this was lower than that of pure EVA. On the other hand, the char yields of IFR–EVA2 and IFR–EVA3 at 800°C were 11.69 and 12.13%, respectively, values that were higher than that of pure EVA.

The previous analysis results illustrate that the IFR–EVA composites had more char residue than the pure EVA. Also, the char residue yield increased with increasing PPMS content.

Macrostructure of the Char Residues with Different IFR–EVA Formulations

Figure 7 shows the exterior macrostructures of the char formed at an incident heat flux of 50 kW/m² with three intumescent formulations (IFR–EVA1, IFR–EVA2, and IFR–EVA3). Samples 1, 2, and 3 represent IFR–EVA1, IFR–EVA2, and IFR–EVA3, respectively. As shown in Figure 7, the intumescent char layer heights of IFR–EVA1, IFR–EVA2, and IFR–EVA3 were about 20, 28, and 43 mm, respectively. This indicates that the char height increased with increasing PPMS content in the composites. The char layer volume increased with increasing char layer height; this helped to inhibit the oxygen and heat penetration into the bottom of the char and delayed the combustion process.
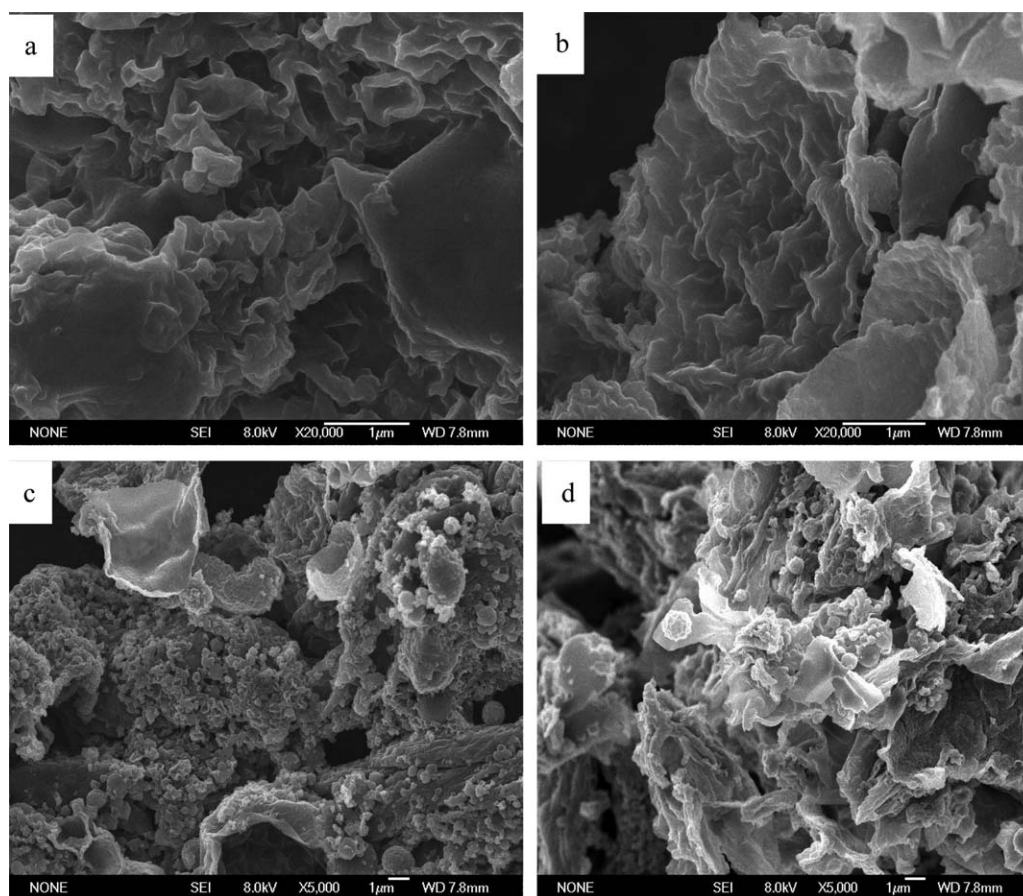

Figure 8. Scanning electron microscopy images of the intumescent char layers after the complete combustion of the IFR–EVA1 and IFR–EVA2 composites.

Compared to the HRR curve of IFR–EVA2 from Figure 3, the flame retardancy of the composite was already very good when the PPMS content was 30%.

Microstructure of Char Residue with Different IFR–EVA Formulations

Figure 8 shows the scanning electron microscopy results of the residual char for the IFR–EVA1 and IFR–EVA2 composites. Figure 8(a,b) presents the lateral surface of the residual char for IFR–EVA1 and IFR–EVA2, respectively, after burning. At the same time, Figure 8(c,d) presents a vertical view of the residual char for IFR–EVA1 and IFR–EVA2, respectively, after burning. Figure 8(a,b) shows that the residual char was stratiform and the coal bed was continuous and pyknotic. Figure 8(c,d) shows that the vertical surface for the residual char after burning was a homogeneous honeycomb structure with some closed pore structures. The formation of this char structure, because of the addition of PPMS into the EVA materials, helped to act as a barrier to suppress the combustion process. Such a kind of char layer could effectively prevent the proliferation of heat and combustible gas. At the same time, oxygen was isolated because of the formed char layer. Accordingly, the intumescent char provided good flame retardancy to EVA. Compared to samples such as IFR–EVA1, with a lower amount of PPMS flame retardant, the sample with a higher PPMS content (e.g., IFR–EVA2) generated a more dense, thick char layer. Thus, the agminated heat and decomposed gas produced during burning found it more difficult to break through char layer, and the flame-retardant effect was more obvious.

CONCLUSIONS

In this study, a single-molecule intumescent fire-retardant, PPMS, was synthesized. The characterization results of PPMS indicated that the synthesized single-molecule intumescent fire retardant was consistent with the chemical structure formula. Then, the IFR–EVA composites were prepared on the basis of EVA resin and PPMS. The LOI and UL 94 rating results illustrate that the PPMS used in EVA improved the flame retardancy of the composites (both the LOI value and UL-94 rating). Cone calorimetry study showed that the addition of PPMS significantly decreased the HRR, THR, and SPR and enhanced the residual char fire performance of the EVA composites. The IFR–EVA3 composite showed the lowest HRR and SPR and the highest char residue; this indicated that the IFR–EVA3 composite had the best flame retardancy. The TG results show that the IFR–EVA composites had more residual char than the pure EVA. The char residue yield increased with increasing PPMS content. The analysis results for the char residue structures also illustrated that the addition of PPMS into the EVA material helped to enhance the fire properties of the char layer and improve the flame retardancy of the EVA composites.

ACKNOWLEDGMENTS

REFERENCES

1. Bourbigot, S.; Fontaine, G. *Polym. Chem.* **2010**, *9*, 1413.

2. Zhang, J.; Delichatsios, M. A.; Bourbigot, S. *Combust. Flame* **2009**, *156*, 2056.

3. Jimenez, M.; Duquesne, S.; Bourbigot, S. *Ind. Eng. Chem. Res.* **2006**, *45*, 4500.

4. Bourbigot, S.; Bras, M. L.; Dabrowski, F.; Gliman, J. W.; Kashiwagi, T. *Fire Mater.* **2000**, *24*, 201.

5. Zhang, F.; Zhang, J.; Jiao, C. *Polym.-Plast. Technol.* **2008**, *47*, 1179.

6. Branca, C.; Blasi, C. D. *Ind. Eng. Chem. Res.* **2002**, *41*, 2107.

7. Morgan, A. B.; Gilman, J. W. *Fire Mater.* **2013**, *37*, 259.

8. Yi, J.; Liu, Y.; Pan, D.; Cai, X. *J. Appl. Polym. Sci.* **2013**, *127*, 1061.

9. Zheng, A.; Xia, Y.; Li, N.; Mao, Z.; Guan, Y. *J. Appl. Polym. Sci.* **2013**, *130*, 4255.

10. Liang, J.; Li, F.; Feng, J. *Polym. Adv. Technol.* **2014**, *25*, 638.

11. Zhang, F.; Zhang, J.; Sun, D. *J. Thermoplast. Compos.* **2009**, *22*, 681.

12. Camino, G.; Costa, L.; Martinasso, G. *Polym. Degrad. Stab.* **1989**, *23*, 359.

13. Delobel, R.; Bras, M. L.; Ouassou, N. F. *J. Fire Sci.* **1990**, *8*, 85.

14. Camino, G.; Martinasso, G.; Costa, L. *Polym. Degrad. Stab.* **1990**, *27*, 285.

15. Camino, G.; Luda, M. P. Fire Retardancy of Polymers: The Use of Intumescence; Royal Society of Chemistry: Cambridge, United Kingdom, **1998**; p 49.

16. Bras, M. L.; Bourbigot, S. Fire Retardancy of Polymers: The Use of Intumescence; Royal Society of Chemistry: Cambridge, United Kingdom, **1998**; p 65.

17. Liu, Y.; Yi, J. S.; Cai, X. F. *J. Appl. Polym. Sci.* **2012**, *124*, 1475.

18. Alongi, J.; Frache, A.; Gioffredi, E. *Fire Mater.* **2011**, *35*, 383.

19. Bras, M. L; Bourbigot, S. *J. Mater. Sci.* **1999**, *34*, 5777.

20. Liu, H.; Xiong, Y.; Xu, W.; Zhang, Y.; Pan, S. *J. Appl. Polym. Sci.* **2012**, *125*, 1544.

21. Doğan, M.; Bayramlı, E. *Polym. Adv. Technol.* **2011**, *22*, 1628.

22. Jimenez, M.; Duquesne, S.; Bourbigot, S. *Polym. Adv. Technol.* **2012**, *23*, 130.

23. Babrauskas, V. *Fire Mater.* **1984**, *8*, 81.

24. Costa, F. R.; Wagenknecht, U.; Heinrich, G. *Polym. Degrad. Stab.* **2007**, *92*, 1813.

25. Usta, N. *J. Appl. Polym. Sci.* **2012**, *124*, 3372.